Appendix
"Deep mutational scanning of the *Neisseria meningitidis* major pilin reveals the importance of the pilus tip in adhesion"
P. Kennouche, *et al.*

CONTENTS

I. GENERAL PRINCIPLE OF THE MODELING

To estimate the hydrodynamic forces and torque on a pilus and the probability for the pilus to adhere to endothelial cells along its side, we consider a fluctuating Brownian rigid rod with one of its ends attached to a plane under a shear flow as described in Supplementary Figure 1(a). The Brownian rod representing a pilus has the length $l \simeq 2\ \mu$m and the radius $a \simeq 3$ nm, and is pivoting on the rod-plane junction which experimentally corresponds to the junction of the pilus and the endothelial membrane. We denote by $\theta(t)$ the deflected angle of the rod from the vertical position at time t, which is a fluctuating variable around an equilibrium position θ_0. The equilibrium angle θ_0 of the rod is determined by the competition between the hydrodynamic torque from the external flow and the restoring torque from the pilus-membrane junction. We assume $\theta_0 = 0$ without any external forces and that the restoring torque at the junction behaves as $-A\theta(t)$, where A is a constant. The value of A gives the idea of physical properties of cell membranes and pili attachment. The equilibrium position θ_0 increases as a function of the strength of the applied external flow. By introducing the s-axis, we parametrize the rod by the distance s from the junction which is comprised between 0 and l. The deformation of the pilus is neglected because the length of the pili in our experiment $l \simeq 2\ \mu$m is more than two times smaller than their persistence length $\sim 5\ \mu$m [1] and, even if not negligible, we can also regard the deformation as incorporated into the effective restoring torque term.

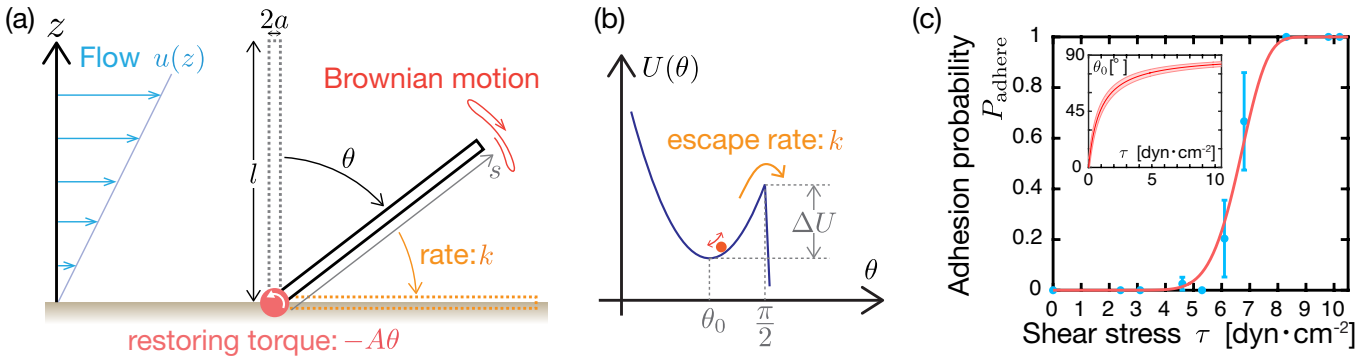

Supplementary Figure 1. (a) Schematic of the model on a fluctuating pilus with one end adhering to the plane under a shear flow. Due to its Brownian motion, the rod stochastically adheres to the plane along its side at the rate k. (b) Potential shape $U(\theta)$ of the Langevin dynamics corresponding to (a). A fluctuating red ball representing the rod has to overcome the energy barrier ΔU in order to reach $\theta = \frac{\pi}{2}$ and escape from the potential well. (c) Probability for pili to newly adhere along their side during the application of the shear flow for the period of $t_{\rm flow} = 30$ s. Experimental data (blue circles) are fitted by eq. (13) (red curve). Error bars: standard errors. Inset: Theoretical values of the equilibrium angle θ_0 calculated from eq. (9) and the fitted value of A. The shaded area represents the standard deviation $\sqrt{k_BT/(A + \frac{2}{\pi}\alpha\tau)}$ of the equilibrium distribution of θ for $\theta < 2/\pi$, $P(\theta) \propto \exp(-U(\theta)/k_BT)$, which gives the idea of fluctuations.

II. HYDRODYNAMIC FORCES AND TORQUE APPLIED ON THE PILUS

We apply the slender body theory [2] for calculating hydrodynamic effects on the rod because $a \ll l$ holds. Under an external flow with the profile $u(z)$, the slender body theory gives the local drag force densities $f_\parallel(s)$ and $f_\perp(s)$ at the position s on the rod as,

$$f_\parallel(s) = \frac{2\pi\eta}{\ln(l/a) - \frac{3}{2} + \ln 2} u_\parallel(z), \tag{1}$$

$$f_\perp(s) = \frac{4\pi\eta}{\ln(l/a) - \frac{1}{2} + \ln 2} u_\perp(z), \tag{2}$$

where η is the viscosity of the fluid, and $\parallel$ and $\perp$ denote components parallel and perpendicular to the rod respectively. Because experimentally we are only interested in the dynamics very close to the plane compared with the channel height $h = 400\ \mu$m ($0 \le z \le l = 2\ \mu\text{m} \ll h = 400\ \mu$m), this ensures a linear flow profile as $u(z) \simeq \frac{\partial u}{\partial z}\big|_{z=0} z = \frac{\tau}{\eta} z = \frac{\tau}{\eta} s\cos\theta$, where τ is the shear stress acting on the plane. Owing to the linearity of low-Reynolds-number flows, we obtain the total hydrodynamic forces $F_\parallel$, $F_\perp$ and the hydrodynamic torque T_{hydro} on the rod as functions of the angle $\theta(t)$ as follows:

$$F_\parallel(\theta) = \int_0^l f_\parallel(s)\cdot \mathrm{d}s = \frac{\pi l^2 \sin\theta\cos\theta}{\ln(l/a) - \frac{3}{2} + \ln 2}\tau \tag{3}$$

$$F_\perp(\theta) = \int_0^l f_\perp(s)\cdot \mathrm{d}s = \frac{2\pi l^2 \cos^2\theta}{\ln(l/a) - \frac{1}{2} + \ln 2}\tau \tag{4}$$

$$T_{\text{hydro}}(\theta) = \int_0^l l \times f_\perp(s)\cdot \mathrm{d}s = \frac{\frac{4}{3}\pi l^3 \cos^2\theta}{\ln(l/a) - \frac{1}{2} + \ln 2}\tau = \alpha\tau\cos^2\theta, \tag{5}$$

where we defined a constant $\alpha := \frac{\frac{4}{3}\pi l^3}{\ln(l/a) - \frac{1}{2} + \ln 2}$ for simplicity.

From the experimental values, $l \simeq 2\ \mu$m, $a = 3$ nm, and $\tau \simeq 10.0\ \text{dyn}\cdot\text{cm}^{-2}$ at the maximum, the maximal hydrodynamic forces on the pilus are estimated as $F_\parallel(\theta) \le F_\parallel(\theta = \frac{\pi}{4}) \simeq 1.1$ pN for the streching force and $F_\perp(\theta) \le F_\perp(\theta = 0) \simeq 3.8$ pN for the perpendicular force, which are two orders of magnitude smaller than the force required for the conformational changes of pili ~ 100 pN [3] as discussed in the main text.

III. ADHESION PROBABILITY

By using the hitherto obtained hydrodynamic torque and the assumption on the restoring torque, the fluctuating dynamics of the rod for $\theta < \frac{\pi}{2}$ is described by an overdamped Langevin equation,

$$\gamma\frac{\mathrm{d}\theta}{\mathrm{d}t} = -A\theta + \alpha\tau\cos^2\theta + \xi(t), \tag{6}$$

$$\langle \xi(t_1)\xi(t_2)\rangle = 2\gamma k_B T\delta(t_2 - t_1), \tag{7}$$

where k_B is the Boltzmann constant, T is the absolute temperature, $\xi(t)$ is a white Gaussian noise with zero mean, and γ is the hydrodynamic friction coefficient for the rotation around the junction that can be similarly calculated by the slender body theory as $\gamma = \frac{\frac{4}{3}\pi\eta l^3}{\ln(l/a) - \frac{1}{2} + \ln 2}$. We assume that as soon as θ reaches $\frac{\pi}{2}$ the rod is tightly trapped and irreversibly adheres to the plane. The equilibrium position θ_0 satisfies,

$$0 = -A\theta_0 + \alpha\tau\cos^2\theta_0. \tag{8}$$

Since we are only interested in the region $0 \lesssim \theta \le \frac{\pi}{2}$, we apply approximation $\cos^2\theta \approx 1 - \frac{2}{\pi}\theta$ and obtain, as a function of τ,

$$\theta_0 \approx \frac{\alpha\tau}{A + \frac{2}{\pi}\alpha\tau}. \tag{9}$$

By applying this approximation, the dynamics of the rod can be written by using an effective potential $U(\theta)$ as,

$$\gamma\frac{\mathrm{d}\theta}{\mathrm{d}t} = -\frac{\partial U(\theta)}{\partial\theta} + \xi(t), \tag{10}$$

$$U(\theta) = \begin{cases} \frac{1}{2}(A + \frac{2}{\pi}\alpha\tau)(\theta-\theta_0)^2 + \text{const.} & (\theta \le \frac{\pi}{2}) \\ -\infty & (\theta > \frac{\pi}{2}). \end{cases} \tag{11}$$

Because the energy barrier $\Delta U := U(\frac{\pi}{2}) - U(\theta_0)$ needs to be overcome by thermal fluctuations so that the rod reaches the plane as depicted in Supplementary Figure 1(b), the probability per unit time k for the rod to newly adhere on the plane (the switching rate from the freely diffusing state to the adherent state) can be estimated from the Kramers escape rate for a cusp-shaped metastable potential [4] as,

$$k = \frac{U''(\theta_0)}{2\pi\gamma}\sqrt{\frac{\pi\Delta U}{k_BT}}\exp\left[-\frac{\Delta U}{k_BT}\right] = \frac{1}{2\gamma}\sqrt{\frac{\pi A^2}{8k_BT}\left(A+\frac{2}{\pi}\alpha\tau\right)}\exp\left[-\frac{\pi^2A^2}{8k_BT}\frac{1}{A+\frac{2}{\pi}\alpha\tau}\right]. \tag{12}$$

Thus the probability for the pilus to be adherent on the endothelial cells after the period of time t_{flow} is estimated as,

$$P_{\mathrm{adhere}}(\tau) = 1 - \mathrm{e}^{-kt_{\mathrm{flow}}} = 1 - \exp\left[-\frac{t_{\mathrm{flow}}}{2\gamma}\sqrt{\frac{\pi A^2}{8k_BT}\left(A+\frac{2}{\pi}\alpha\tau\right)}\exp\left(-\frac{\pi^2A^2}{8k_BT}\frac{1}{A+\frac{2}{\pi}\alpha\tau}\right)\right], \tag{13}$$

where A is the only unknown parameter that is used for fitting this curve to the experimental data.

IV. FITTING TO THE EXPERIMENTAL DATA

We fitted the theoretical curve eq. (13) to the experimentally measured probabilities for pili to newly adhere along their side. In our experimental protocol, the adhesion probability as a function of shear stress τ was measured successively by applying shear flows with different shear stress on the same pili for the period of $t_{\mathrm{flow}} = 30$ s each. Since we increased the shear stress τ stepwise and the pili irreversibly adheres to the endothelial cells without any possibility of detachment, the number of remaining nonadherent free pili N_i after the application of the i-th shear flow gradually decreases from the initial value N_0 as the increase of i. Therefore, the probability for nonadherent pili to *newly* adhere to the endothelial cells during the application of the i-th flow is given by $P_i = 1 - \frac{N_i}{N_{i-1}}$, which is plotted in Fig. 5C in the main text and Supplementary Figure 1(c). We note that, for the high shear stress region $\tau > 9.0\ \mathrm{dyn\cdot cm^{-2}}$, all the pili had already adhered along their side before applying such high shear stress in all our three trials and thus P_i cannot be defined experimentally. Nonetheless, in Supplementary Figure 1(c), we kept our experimental measurement points in $\tau > 9.0\ \mathrm{dyn\cdot cm^{-2}}$ by setting the probability $P_i = 1$. We fitted $P_{\mathrm{adhere}}(\tau)$ in eq. (13) to P_i via the single fitting parameter A using the data points only in $\tau < 9.0\ \mathrm{dyn\cdot cm^{-2}}$.

For fitting, we used the following values for the known parameters: $T = 273{+}37 = 310$ K, $k_B = 1.38{\times}10^{-23}\ \mathrm{J\cdot K^{-1}}$, $l = 2\ \mu$m, $a = 3$ nm, $\alpha = \frac{\frac{4}{3}\pi l^3}{\ln(l/a)-\frac{1}{2}+\ln 2} = 5.00\ \mu\mathrm{m}^3$, $\eta = 0.72$ mPa$\cdot$s for cell culture media with 10% serum [5], $\gamma = \frac{\frac{4}{3}\pi\eta l^3}{\ln(l/a)-\frac{1}{2}+\ln 2} = 3.60\ \mathrm{pN\cdot nm\cdot s\cdot rad^{-1}}$, and $t_{\mathrm{flow}} = 30$ s. The best fit of eq. (13) to P_i gives the estimate of $A = (2.909 \pm 0.017) \times 10^{-1}\ \mathrm{pN\cdot\mu m\cdot rad^{-1}}$ ($\pm$: standard error of fitting). This fitted curve is shown in Fig. 5C in the main text and Supplementary Figure 1(c). To make the probability map in Figure 5E in the main text, ΔU was replaced with $\Delta U(\theta) = U(\theta) - U(\theta_0)$ and we calculated the following generalized escape rate $k(\theta)$ and probability by using the parameter obtained by the fitting:

$$P(\theta,\tau) = 1 - \mathrm{e}^{-k(\theta)t_{\mathrm{flow}}} = 1 - \exp\left[-t_{\mathrm{flow}}\frac{U''(\theta_0)}{2\pi\gamma}\sqrt{\frac{\pi\Delta U(\theta)}{k_BT}}\exp\left[-\frac{\Delta U(\theta)}{k_BT}\right]\right]. \tag{14}$$

The values of this map at $\theta = \pi/2$ are by definition the same as $P_{\mathrm{adhere}}(\tau)$ that are plotted in in Fig. 5C in the main text and Supplementary Figure 1(c).

In conclusion, the fact that the theoretical curve with only one fitting parameter quantitatively explains the experimental data supports the simple physical picture that the shear flow tilts the Brownian rod resulting in the

exponentially higher probability of adhesion along its side.

---

[1] Jeffrey M. Skerker and Howard C. Berg, Direct observation of extension and retraction of type IV pili, *Proceedings of the National Academy of Sciences USA*, **98**, 6901–6904 (2001).

[2] R. G. Cox, The motion of long slender bodies in a viscous fluid Part 1. General theory, *Journal of Fluid Mechanics*, **44**, 791–810 (1970).

[3] Nicolas Biais, Dustin L. Higashi, Jasna Brujić, Magdalene So, and Michael P. Sheetz, Force-dependent polymorphism in type IV pili reveals hidden epitopes, *Proceedings of the National Academy of Sciences USA*, **107**, 11358–11363 (2010).

[4] Peter Hänggi, Peter Talkner, and Michal Borkovec, Reaction-rate theory: fifty years after Kramers, *Review of Modern Physics*, **62**, 251–341 (1990).

[5] Ibidi, Application Note, AN 11: Shear Stress and Shear Rates, `https://ibidi.com/img/cms/support/AN/AN11_Shear_stress.pdf`